Mazarío-Santa-Pau, J.; Raad, Z.; Concepción Heydorn, P.; Cerdá-Moreno, C.; Domine, ME. (2020). Pd supported on mixed metal oxide as an efficient catalyst for the reductive amination of bio-derived acetol to 2-methylpiperazine. Catalysis Science & Technology. 10(23):8049-8063. https://doi.org/10.1039/d0cy01423k

Pd supported on Metal Mixed Oxide as an Efficient Catalyst for the Reductive Amination of Bio-derived Acetol to 2-Methylpiperazine

Jaime Mazaríoª, Zaher Raadª, Patricia Concepciónª, Cristina Cerdá-Morenoª and Marcelo E. Domineª,*

ª *Instituto de Tecnología Química (UPV-CSIC), Universitat Politècnica de València, Consejo Superior de Investigaciones Científicas, Avda. de los Naranjos s/n, 46022 Valencia, Spain*

* mdomine@itq.upv.es

Abstract

An efficient process for synthesizing a high added-value N-heterocycle (2-methylpiperazine, 2-MP) via reductive amination of hydroxyacetone or acetol (product of the selective dehydration of glycerol) with ethylenediamine by using Pd supported catalysts under mild reaction conditions is here presented. Catalysts based on Pd nanoparticles supported on metallic oxides and mixed oxides were prepared and characterized by ICP analysis, XRD, HR-TEM, and NH_3-TPD, among others. Catalytic activity comparisons of Pd-based materials (also including commercial references) were done and obtained results correlated with metal particle morphology (analyzed by CO-FTIR) and its ability to activate C=N bond. Best results were attained with Pd/TiO_2-Al_2O_3, and Pd/ZrO_2-Al_2O_3, the former yielding >80% of 2-MP. The Pd/TiO_2-Al_2O_3 catalyst successfully enables the activation of the imine group (C=N), due to a larger number of unsaturated Pd sites in its nanoparticles, while keeping a proper acidity to effectively and selectively carry out the reductive cyclo-amination reaction even with lower catalyst loadings. This research work offers a new and sustainable catalytic route for the synthesis of organo-nitrogen compounds taking advantage of renewable raw materials (i.e. acetol) as a carbon source and using efficient Pd supported catalysts.

Keywords: *biomass derivatives, glycerol, acetol, piperazine, reductive amination, heterogeneous catalysts, palladium nanoparticles, metal oxides.*

1. Introduction.

During the last decades, the increasing use of fossil resources to produce fuels and chemical has contributed to the constant increase in the prices of this shrinking resources, as well as to the augmentation of greenhouse gases (GHG) emissions and their levels in the atmosphere. Thus, the conversion of renewable raw materials in fuels and, more specifically, in chemicals, is becoming more and more attractive. In this sense, biomass outstands as the only renewable source of organic carbon to produce chemicals.[1,2] In particular, the possibilities offered by the oxygenated functionalities of biomass-derived molecules for their transformation into organonitrogen chemicals has recently been acknowledged.[3] Nonetheless, a path seldom explored so far is the transformation of glycerol derivatives into nitrogenated compounds. In this sense, the final objective is to develop an efficient catalytic route to obtain N-heterocycles of piperazine type out of a glycerol selective dehydration product, hydroxyacetone (or acetol), whose continuous production has lately been the object of study of several groups. [4-7] This catalytic route must include the use of heterogeneous catalysts and comply with the Green Chemistry principles.[8]

The piperazine ring is an anthelmintic[9], and can also be found as a building block for a large number of high added value drugs, from antihistamines to antidepressants, being synthesis intermediate chemicals highly valued in organic chemistry.[10] On the other hand, CO_2 capture systems based on amine scrubbing using piperazine derivatives recently caught the attention due to the high energetical and adsorption performances of such technology. Indeed, these systems proved to have very good regeneration ability by thermal swing regeneration, without significant degradation of the scrubbing solvent, good resistance to oxidative degradation, lower volatility, compared to other typical amine-based solvents, and a corrosive-friendly behavior to stainless steel.[11,12]

Nowadays, the most employed commercial route to produce piperazine derivatives consists in the ammonization of either 1,2-dichloroethane or ethanolamine over a Ni-Raney catalyst at 195 ^{o}C and very high H_2 pressures (>130 bar), being the piperazine obtained as a by-product that needs to be separated from the main stream of ethylenediamine, triethylenediamine and other related cyclic and linear nitrogenated compounds.[13] It is noteworthy that 1,2-dichloroethane and ethanolamine are mainly obtained from fossil resources and, in particular, from ethylene.[14,15] As far as the synthesis of 2-methylpiperazine (2-MP) is concerned, old synthetic approaches to this chemical also involved the use of Ni-Raney catalysts in batch

reactors by using N-β-hydroxypropyl-ethylenediamine and hydrogen (at 13 bar and 200 ºC), with moderated yields (≈50 %) and no available data about catalyst recyclability.[16] More recently, other syntheses using heterogeneous catalysts have been described in the literature, standing out a continuous process for the intra-cyclization of N-β-hydroxypropyl-ethylenediamine at 205 ºC and H_2 pressure of 260 over Cu–Cr–Fe/γ-Al_2O_3 ºcatalysts,[17] the same intra-cyclization but over zeolite H-ZSM-5 at 260 ºC,[18] and the intermolecular cyclization of diethanolamine and methylamine to N,N′-dimethylpiperazines and N-methylpiperazines at 300 ºC and high H_2 pressures (80-100 bar) with H-ZSM-5 as catalyst.[19,20] It is also remarkable the obtention of the piperazine ring by condensation-cyclization reactions of diethanolamine with NH_3 in the presence of hydrogen and a catalyst containing Al, Co, Ni, Cu and Sn-oxides working at 200 ºC and H_2 pressure of 200 bar.[21] Nonetheless, and mainly due to the use of harsh reaction conditions, commercial application of these processes is difficult and there is still plenty of room for improvement. Thus, in the current study, the reductive cyclo-amination of acetol in presence of a diamine and a heterogeneous catalyst is proposed as a promising alternative to produce the desired 2-methylpiperazine.

The reductive amination of aldehydes and ketones is an organic reaction, widely used in the synthesis of substituted amines and aromatic and aliphatic N-heterocycles. The proposed mechanism for the reductive amination of carbonyl compounds is detailed in Scheme 1:

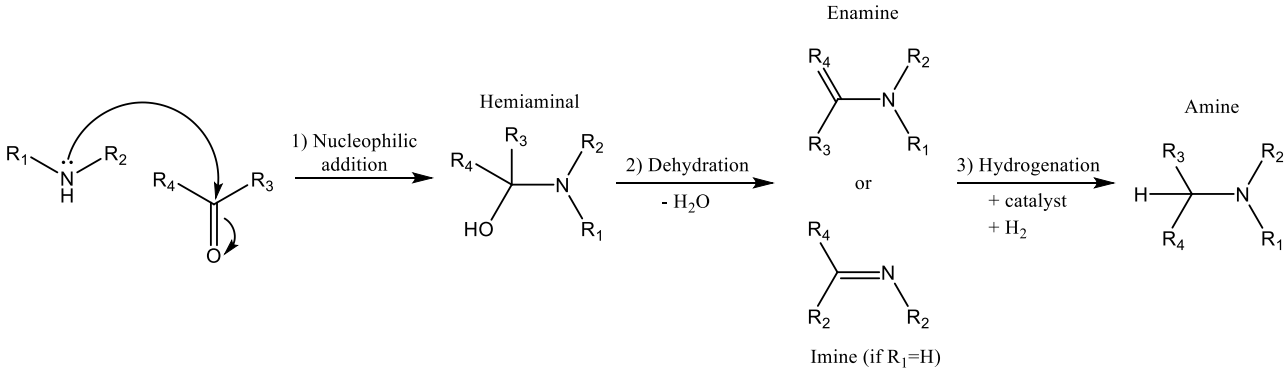

Scheme 1. Reductive amination mechanism for carbonyl-type compounds – Adapted from Refs. [22,23]

If the reactants are aldehydes or ketones, the reaction would include: 1) addition and generation of the intermediate hemiaminal, 2) intermediate imine or enamine dehydration and formation and 3) imine or enamine reduction to obtain the final substituted amine. The enamine or imine reduction is usually the determining step for the reaction rate, since it would compete against

the carbonyl group hydrogenation.[24] In the case of alcohols, the first step would consist in an oxidative dehydrogenation of the alcohol to yield the corresponding carbonyl compound, being this stage the limiting one. This fact explains the low reactivity as well as the high temperatures needed to obtain the substituted amines when using alcohols as the starting oxygenated reactant. [24,25] In our case, the use of hydroxyacetone (or acetol) is proposed. This reactant allows for keeping a compromise between the high reactivity of the di-carbonyl compound (i.e. pyruvaldehyde) and the low reactivity of the glycol (i.e. 1,2-propylen glycol).

The reductive amination of aldehydes and ketones using different reductive agents consisting of boron (i.e. sodium borohydride, sodium triacetoxyborohydride, sodium cyanoborohydride) has been widely studied,[26-28] although the use of these classic reductive agents, as well as that of the acetic acid and other additives constitute important drawbacks that need to be overcome. Besides that, in the last decades, different processes using Fe, Ir or Pd complexes as catalysts and molecular hydrogen as reducing agent have been described, being these ones especially important in the synthesis of chiral amines.[29-31] However, the use of expensive and low efficient catalysts is often found together with the use of quite drastic pressure and temperature conditions, in addition to the disadvantages commonly associated to homogeneous catalysis application. These are the main reasons why the development of novel heterogenous catalysts, capable of carrying out this reaction under moderate conditions with aldehydes, ketones and even β-hydroxyketones is a very attractive path. Some authors already explored this line, being mixed metal oxides and modified zeolites with metallic functions (metal: Cu, Zn, Ni and Co)[32-34] the most broadly used catalysts. In this sense, our group has already reported some auspicious results using catalysts based on noble metals (Au, Pt, Pd) supported on simple oxides and nanostructured materials such as Beta zeolites and MCM-41, proving that the alternative use of such catalytic systems allows working under mild and more sustainable reaction conditions. More precisely, systems using Pd or Pt as metal and Al_2O_3 or MgO as supports are the ones that have produced the best results up to date.[22,23,35] Since then, several examples based on the use of noble metals supported on metal oxides as heterogenous catalysts for reductive aminations have been reported in the literature. For instance, systems such as Pt/TiO_2,[36,37] and $Pt\text{-}MoO_x$,[38] are very effective as catalysts in reductive amination reactions with ethyl levulinate and levulinic acid, respectively. More recently, Pd supported on magnetite demonstrated to be efficient for the one-pot reductive amination of aldehydes with nitroarenes.[39] These catalysts satisfy the reaction requirements regarding active redox type centers offering, additionally, acid-base centers of moderate strength.

In light of all the above-mentioned, this work wants to set value on the development of a new catalytic route to produce 2-methylpiperazine. In this sense, the use of bio-derived acetol offers a novel alternative for the synthesis of 2-methylpiperazine under moderate conditions through reductive cyclo-amination with ethylenediamine as Nitrogen source. Metallic Pd nanoparticles supported on different simple and mixed metal oxides with high surface area and controlled acid properties will be studied and applied as catalyst. Catalytic activity comparisons by using other metal supported catalysts (also including Pt-based and commercial reference materials) will be done. Deep characterization of Pd-based materials will allow establishing correlations between catalytic performance and physico-chemical properties (Pd nanoparticles size and morphology, H_2 activation and acid capacities, etc.), thus providing new insights into the reductive amination process taking place~~s~~ over these Pd-based catalytic systems. Finally, we take advantage of the outstanding ability of Pd/TiO_2-Al_2O_3 to hydrogenate the C=N functionality to extend the scope of this work via the reductive amination of glyoxal.

2. Experimental

2.1 Materials and reagents

Main reagents, i.e. ethylenediamine (99%) and hydroxyacetone (90%) have been supplied by Sigma-Aldrich, while hydrogen (99.999%) was purchased from Abelló Linde S.A (Spain). Methanol (Scharlau, analytical grade, 99.5%) and high purity water (milliQ water, Millipore) have been used as reaction solvents. Additionally, a glyoxal solution (40wt.%, aq.) was selected to extend the scope of some catalysts. As an internal standard for carbon balance purposes, a 1 wt% solution of chlorobenzene (Sigma-Aldrich, 99.90%) in methanol was used to dilute the samples. Finally, 2-methylpiperazine (99.5%, Sigma-Aldrich) allowed the determination of the response factors of the different reagents GC-FID analysis. Commercial 1wt% Pd/Al_2O_3 and 1wt% Pt/Al_2O_3 catalysts were purchased from Sigma-Aldrich and used in the preliminary tests. γ-Al_2O_3 (Sigma-Aldrich, 99.0%), TiO_2 nanoactive (NanoScale Corporation, 99%), MgO nanoactive plus (NanoScale Corporation, 99%) and ZrO_2 oxides (tetragonal and monoclinic phases, both from Chempure, 99%) were used as supports for catalyst preparation. Mixed oxide synthesis was achieved using $Al(NO_3)_3{\cdot}9H_2O$ (Sigma-Aldrich, 99.5%), $TiOCl_2{\cdot}HCl$ (Sigma Aldrich solution, ~15wt% Ti basis) and $ZrOCl_2{\cdot}8H_2O$ (Sigma-Aldrich, 99.5%) as precursors. Ammonia solution (Sigma-Aldrich, 25vol%) was selected as precipitant agent, while $Pd(NH_3)_4Cl_2{\cdot}H_2O$ (Sigma-Aldrich, 99.00%) was chosen as metallic precursor.

2.2 Catalyst preparation

Commercial Al_2O_3, MgO, TiO_2 and ZrO_2 supports were calcined before use at 250 ºC (under air, 2h, 2 ºC/min), whereas mixed metal oxides were prepared by co-precipitation in ammonia medium (TiO_2-Al_2O_3, TiO_2-ZrO_2 and ZrO_2-Al_2O_3). Appropriate amounts of the metallic precursors (30 mmol of each precursor to attain a molar ratio M_1:M_2 = 1) were dissolved in 300 ml of water, being stirred for 10 minutes. Afterwards, an ammonia aqueous solution (25vol%.) was added dropwise (1000 ml/h) until the pH was approximately 9, and the solution was stirred for another 15 minutes. After that, the precipitate was aged during 12 h at 60 ºC, and then filtered and washed with water. The solid obtained was dried at 100 ºC during 24 h and calcined at 500 ºC during 3 h (under air, 2 ºC/min) to obtain the corresponding metallic mixed oxide. It is relevant to notice that ZrO_2 support corresponds to a physical blend of 60/40 in weight of monoclinic/tetragonal commercial zirconia. The incorporation of palladium onto every support was carried out by incipient wetness impregnation method using an aqueous solution of $Pd(NH_3)_4Cl_2 \cdot 6H_2O$ in adequate concentrations to get a metal loading of ≈1wt% in the final solid. Impregnated solids were dried in a stove at 100 ºC during 24 h, and, afterwards, all the catalytic systems were calcined (450 ºC for Al_2O_3 and MgO; and 400 ºC for TiO_2, ZrO_2 and mixed oxides) (under air, 3 ºC/min). All the catalysts were thermally treated at 400 ºC (3 ºC/min) under a H_2 flow of 100 ml/min during 2 h prior to their use in catalytic experiments.

2.3 Catalyst characterization

Crystalline phase identification was carried out by X-ray diffraction using a PANalitical Cubix Pro diffractometer (CuK_α radiation), at a scan rate of 2 min^{-1}, operating at 40 kV and 35 mA, provided with a variable divergence slit and working in fixed irradiated area mode. Palladium content of fresh and used catalysts and metal ratios of mixed oxide-based catalysts were determined using a Varian 715-ES ICP (Inductively Coupled Plasma - Optical Emission Spectrometer) equipment after solid dissolution in HNO_3/HCl/HF aqueous solution (1:1:1 vol.), except for MgO (same but without HF). The instrument was previously calibrated for Pd, Al, Ti, Zr and Mg measurements. Possible organic matter deposition during reactions was checked by means of elemental analyses (EA) of spent catalysts carried out in a Fisons EA1108CHN-S apparatus, using sulfanilamide as the reference. Liquid nitrogen adsorption experiments were measured by using N_2 adsorption isotherms at -196 ºC, in a Micromeritics flowsorb apparatus.

Specific surface areas were calculated by applying the Brunauer–Emmet–Teller (BET) model over the range P/P^0 = 0.05–0.25 of the isotherm.

High Resolution Electronic Transmission Microscopy (HR-TEM) study of fresh and used catalysts was performed in a Jeol JEM-2100F equipment, working at 200 kV. HR micrograph analysis, lattice spacing, First Fourier Transform (FFT) and phase interpretation, were done using the Gatan Digital Micrograph software (Gatan Inc.) and the Java version of the Electron Microscope Software (JEM). Mixed metal oxide homogeneity has been checked by X-ray energy-dispersive spectroscopy to obtain the elemental mapping using a JEOL 6300 Scanning Electron Microscope (SEM) equipped with an Oxford LINK ISIS detector. Mapping images were obtained with a focused beam of electrons (20 kV) and a counting time of 50-100s.

Ammonia Thermo-Programmed Desorption (NH_3-TPD) profiles were obtained after a previous conditioning step of the calcined catalysts under a flow of He (35 ml/min) from room temperature to 500 ºC (10 min); after cooling up to 100 ºC, adsorption of ammonia flow (10 min) was performed at constant temperature, followed by a last cleaning step using a He flow (35 ml/min), allowing for elimination of the physiosorbed ammonia. Finally, Thermo-Programmed Desorption is carried out by heating the samples from 100 to 500 ºC at a heating rate of 10 ºC/min. The evolved ammonia was analyzed using an on-line gas chromatograph (Shimadzu GC-14A) provided with a TCD and previously calibrated by measuring the corresponding signals of the thermal decomposition of known amounts of hexaamine-nickel(II) chloride $[Ni(NH_3)_6]Cl_2$.

Pd metal dispersion of the sample was estimated from CO adsorption using the double isotherm method on a Quantachrome Autosorb-1C equipment. Prior to adsorption, 300 mg of the sample (0.45-0.8 mm) were reduced in flowing hydrogen by using the same reduction temperature applied before for catalysts (i.e. 400 ºC during 2 h and 3 ºC/min). After reduction, samples were degassed at 1333 x 10^{-3} Pa during 2 h at 400 ºC, and then, temperature lowered at 35 ºC. Next, pure CO was admitted and the first adsorption isotherm (i.e. the total CO uptake) was measured. After evacuation at 35 ºC, the second isotherm (i.e. the reversible CO uptake) was taken. The amount of chemisorbed CO was calculated by subtracting the two isotherms. The pressure range studied was 0.5-11 x 10^4 Pa. Pd dispersion was calculated from the amount of irreversibly adsorbed CO, assuming a stoichiometry Pd/CO = 1.

IR spectra of adsorbed CO were recorded at 25 ºC with a Nexus 8700 FTIR spectrometer using a DTGS detector and acquiring at 4 cm^{-1} resolution. An IR cell allowing for in situ treatments

in controlled atmospheres and temperatures from 25 to 500 ºC has been connected to a vacuum system with a gas dosing facility. For IR studies the samples were pressed into self-supported wafers and in situ reduced at 250 ºC in a H_2 flow (10 ml min^{-1}) for 1.5 h followed by evacuation at 10^{-4} mbar at 300 ºC for 1h. After activation, the samples were cooled down to 25 ºC under dynamic vacuum conditions followed by CO dosing at increasing pressure (0.4-8.5 mbar). IR spectra were recorded after each dosage.

Hydrogen/deuterium (H_2/D_2) exchange experiments were carried out in a flow reactor in order to study the capability for H_2 activation of the catalysts. The feed gas consisted in a mixture of H_2 (4 ml/min), D_2 (4 ml/min), and Ar (17 ml/min), and the total weight of catalyst was 0.4 mg. The reactor outlet was coupled with a mass spectrometer (Balzer, Tecnovac), working in the multi ion detection mode (MID) and recording the mass signal (m/Z) of 2 (H_2), 3(HD) and 4(D_2). The samples were "in situ" reduced in a H_2 flow, following the same procedure for catalyst activation prior to their use in catalytic tests. After sample activation, the temperature was decreased to 25 ºC in a flow of Ar (25 ml/min), and once the mass signal was stable, the Ar flow was switched to the H_2/D_2/Ar reaction mixture. After 30 min stabilization at 25 ºC, the temperature was sequentially increased to 60 ºC, 90 ºC and 120 ºC, maintaining at each temperature for at least 30 min.

2.4 Catalytic tests

Reductive cycle-amination reactions were carried out in a "batch" type micro-reactor of 6 ml with a probe for sampling and a pressure gauge for pressure measurements. Reproducibility of the system was carefully evaluated with the commercial catalyst (Figure S11, ESI). The amount of sample collected was always between 0.040 and 0.050 g and kinetic experiments were done by avoiding removing more than 15% of the total weight of the reaction mixture. A test to discard any effect of the sampling on the catalytic activity can be found at the ESI (Table S1). The reactor was purged twice with 10 bars of N_2 before feeding it with H_2. The H_2 pressure in the system was maintained practically constant during all the experiment by recharging H_2 every 30 minutes. Typically, reactions were carried out in presence of 13 bar of H_2, at 90 ºC during 7 h and at stirring rate of 800 rpm. In preliminary experiments, 0.318 g of acetol (3.8 mmol), 0.227 g of ethylenediamine (3.8 mmol) and 0.056 g of catalyst were added at the same time, in presence of 1.250 g of solvent (methanol). Afterwards, an improved protocol where acetol is not initially introduced in the batch reactor and involving slow and continuous addition

of it at an addition rate of 100 µl/h was applied. In all cases, total conversion (*X*), selectivities (S_i) and yields (Y_i) of the different products *"i"*, have been estimated through GC analysis of the different aliquots collected at different reaction times ("*t*"), see equations 1, 2, 3, and 4), taking ethylenediamine as the reference reactant. A few experiments were also done by using water instead of MeOH as the reaction solvent.

$$X^t(mol.\%) = \frac{n^0_{ethylenediamine} - n^t_{ethylenediamine}}{n^0_{ethylenediamine}} \cdot 100 \quad \text{(eq. 1)}$$

$$S_i^t(mol.\%) = \frac{n_i^t}{n^t_{total\ products}} \cdot 100 \quad \text{(eq. 2)}$$

$$Y_i^t(mol.\%) = \frac{n_i^t}{n^0_{ethylenediamine}} \cdot 100 \quad \text{or} \quad Y_i^t(mol.\%) = \frac{X^t \,.\, S_i^t}{100} \; if\; CB > 95\% \quad \text{(eq. 3 and 4)}$$

TON (Turnover number) was also calculated and defined as the mol of 2-methylpiperazine produced per mol of metal present in the initial solid catalyst at a given reaction time (see equation 5). Final carbon balances were calculated for each reaction, considering the total amount of products detected by GC analysis along with the remnant ethylenediamine (see equation 6).

$$TON = \frac{n^f_{2-methylpiperazine}}{n^0_{METAL}} \quad \text{(eq. 5)}$$

$$CB(mol.\%) = \frac{\left[(n^0_{ethylenediamine} - n^f_{ethylenediamine}) \cdot 3\ C\ atoms\right] + \sum(n^f_{product} \cdot X\ C\ atoms)}{n^0_{ethylenediamine} \cdot 3\ C\ atoms} \cdot 100 \text{ (eq. 6)}$$

Being *X* de total number of C atoms in the molecules corresponding to the different by-products coming from ethylenediamine.

It is essential to point out that the reaction between ethylenediamine and acetol to give rise to the corresponding cyclic and linear imines is thermal and does not require either hydrogen or a catalyst. Consequently, most of the catalytic comparisons herein presented work with the yield to 2-MP as the comparative parameter, if operating with values not exceeding 80% by much, being this a measure of the "effective activity" of the catalyst.

GC analyses of the reaction mixtures were carried out using a 3900-Varian GC equipped with a FID detector and a capillary column (HP-5, 30 m length). Product identification was done by GC–MS (Agilent 6890N GC System coupled with an Agilent 5973N mass detector).

2.5 Reusability tests

In addition, some experiments were done using water instead of MeOH as reaction solvent and some recyclability tests were done for selected catalysts. Four complementary and successive catalytic tests were performed; the first three ones correspond to the direct separation and recovery of the solid catalyst after reaction through filtration, followed by a thorough washing using MeOH (3 mL, 10 min) and final catalyst recovery by centrifugation. Thereafter, an additional (fourth) catalytic cycle was done, involving the same steps previously described together with a catalyst regeneration step under the same conditions employed for sample activation prior to reaction usage (i.e. 400 ºC, under H_2 flow during 2 h, 3 ºC/min). It is Worthing to note that, in order to avoid any catalyst losses during the consecutive recycles, and the subsequent scaling down of the other reactants involved in the reaction, a pyramidal scheme was followed with four repetitions for the first use, three for the second one, etc., thereby guaranteeing to have 56 mg of catalyst per reaction in all cases.

3. Results and discussion

3.1 Physico-chemical characterization of catalysts.

The textural and physico-chemical analyses of catalysts based on Pd supported on simple metal oxides proved that they present quite similar surface areas (≈150 m^2/g) and average metallic particle sizes between 4- and 8 nm (measured by TEM), with the only exception of Pd/MgO sample (surface area >200 m^2/g and average particle size = 14 nm) (Table 1). It can also be observed that the method applied for metallic mixed oxide synthesis allows for obtaining materials with improved properties, i.e. surface areas ≥250 m^2/g, and average particle sizes around 2-3 nm, as opposed to any of the simple oxides.

Table 1. Main textural and physico-chemical properties of Pd-supported materials.

Material	Pd (wt%)[a]	Surface area (m^2/g)[b]		Particle size (nm)	
		Catalyst	Support	TEM[c]	CO[d]
Pd/TiO_2	1.2	120	148	4	8
Pd/Al_2O_3	1.0	135	138	8	4
Pd/ZrO_2	1.1	158	180	5	4
Pd/MgO	1.0	194	226	10	n/d
Pd/TiO_2-Al_2O_3	1.0	318	351	1	3
Pd/TiO_2-ZrO_2	1.1	257	292	4	4
Pd/ZrO_2-Al_2O_3	0.9	215	247	4	2

[a] Pd content and chemical composition measured by ICP. [b] Values calculated from N_2 adsorption isotherms (BET method). [c] Average diameter of Pd nanoparticles calculated from TEM measurements of, at least, 100 particles. [d] Average diameter of Pd nanoparticles evaluated by CO chemisorption, with the stoichiometry being Pd:CO = 1:1.

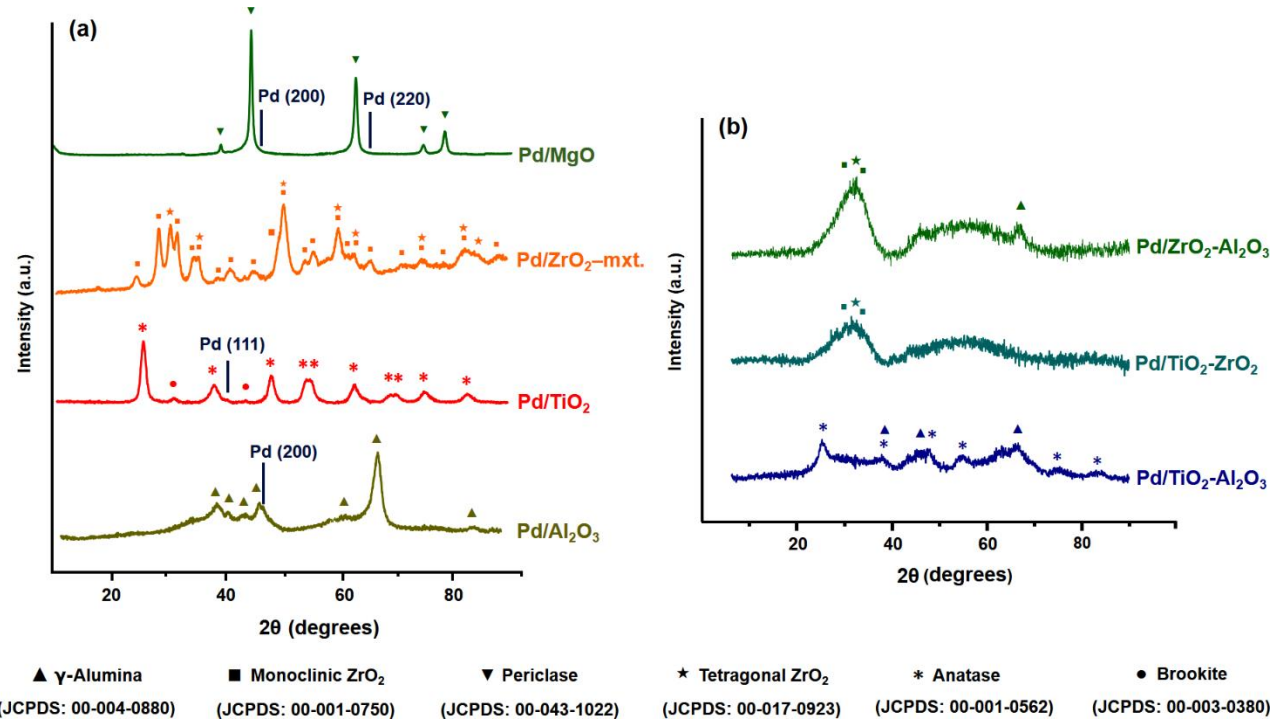

Figure 1. X-ray diffraction patterns of Pd supported materials (after reduction): a) Pd/Al_2O_3, Pd/TiO_2, Pd/ZrO_2 and Pd/MgO; b) Pd/TiO_2-Al_2O_3, Pd/TiO_2-ZrO_2 and Pd/ZrO_2-Al_2O_3.

The X-ray diffraction patterns for the various Pd supported on simple oxide materials are shown in Figure 1a. The characteristic peaks for γ-alumina are observed in the reduced Pd/Al_2O_3

material, whose broadness indicates a low level of crystallinity. Additionally, this catalyst hardly presented a very weak peak, characteristic of the Pd^0 species, probably due to the presence of small nanoparticles, relatively well dispersed on the support. The X-ray diffractogram of reduced Pd/MgO sample presented the characteristic diffraction peaks of the periclase phase of MgO, while the diffraction peaks assigned to Pd^0 species cannot be clearly noticed in the Pd/MgO reduced sample. Pd/TiO_2 predominantly showed the anatase phase and a small percentage of brookite. With respect to Pd/ZrO_2, the reduced material presents certain peaks that can be associated to the tetragonal phase and some others that appear because of the characteristic reflections of the monoclinic phase, being almost impossible to distinguish those peaks corresponding to the presence of Pd^0 species.

As for the diffractograms obtained for Pd supported on metallic mixed oxide materials after reduction (Figure 1b), although some peaks showing very low crystallinity and corresponding to single oxide phases have been noticed, the predominant structure in every case is that of an amorphous mixed oxide. This has also been confirmed through EDAX compositional analyzes (see ESI, Figures S1-3), where a very good dispersion is attained for both metals involved in each one of the structures.

Pd supported materials were also analyzed by means of high-resolution transmission electron microscopy (HR-TEM). The images for each one of the catalysts here studied are shown in Figure 2 and 3 for single and mixed oxide-based samples, respectively. The presence of metallic Pd nanoparticles can be appreciated in all of them. Regarding particle size distribution for single oxide-based materials (see ESI, Figure S5), Pd/MgO and Pd/Al_2O_3 show the higher average particles sizes, whereas Pt/ZrO_2-mix sample presents particles sizes values around 4.0-6.0 nm. These Pd particles sizes are slightly above than those observed for Pd/TiO_2-ZrO_2 and Pd/ZrO_2-Al_2O_3 (2.0-4.0 nm), whereas Pd/TiO_2-Al_2O_3 and Pd/TiO_2 samples are the only ones showing a maximum in particle size distribution between 1.0 and 3.0 nm, and also exhibiting particles with sizes below 1.0 nm (see ESI, Figures S5-6). HR-TEM measurements of the catalysts after reuses and further regeneration were also performed. In general, particle size distributions observed for regenerated samples moved towards higher values, and the particles with sizes below the nanometre practically disappear (see ESI, Figures S5-6).

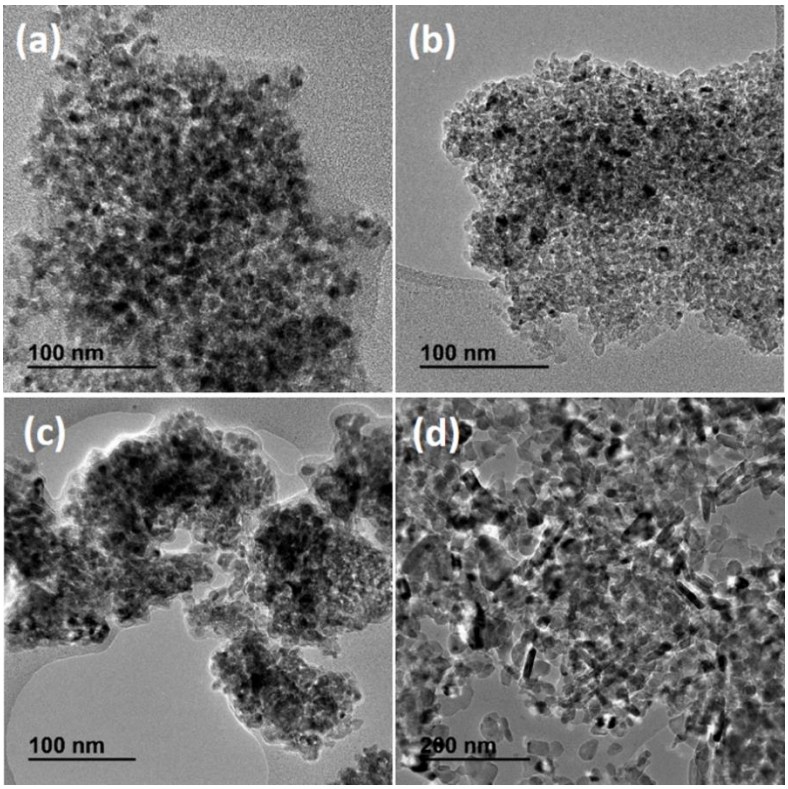

Figure 2. HR-TEM of a) Pd/TiO_2, b) Pd/Al_2O_3, c) Pd/ZrO_2 and d) Pd/MgO (after reduction).

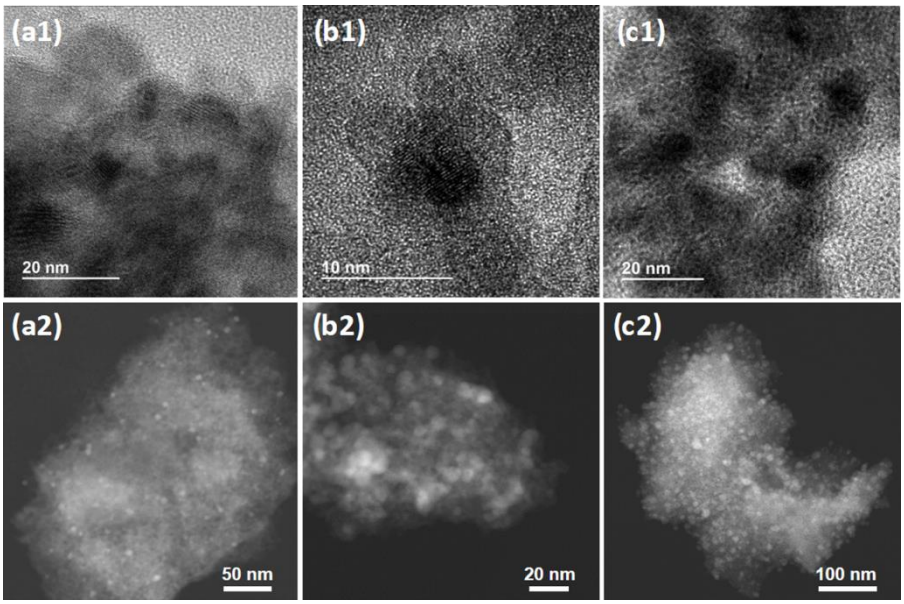

Figure 3. HR-TEM(1) and HR-STEM(2) images of a) Pd/TiO_2-Al_2O_3, b) Pd/TiO_2-ZrO_2 and c) Pd/ZrO_2-Al_2O_3 (after reduction).

In addition, and with the objective of establishing structure-activity relationships for the catalysts herein presented, a study of their acidic properties was carried out through temperature programmed desorption of ammonia (TPD-NH_3). Table 2 shows the total amount of ammonia adsorbed for each catalyst, except for Pd/MgO considered as non-acidic material and with negligible ammonia adsorption. Thus, important differences were established between the different materials, whose total acidity can be ordered as follows: Pd/ZrO_2 > Pd/TiO_2-Al_2O_3 > Pd/TiO_2 > Pd/ZrO_2-Al_2O_3 > Pd/TiO_2-ZrO_2 > Pd/Al_2O_3. This finding might influence the catalytic properties of the different materials in the reductive amination reaction, which will be discussed in the next sections.

Table 2. Ammonia adsorption on the different catalysts.*

Catalyst	**Pd/Al_2O_3**	**Pd/TiO_2-ZrO_2**	**Pd/TiO_2**	**Pd/ZrO_2-Al_2O_3**	**Pd/TiO_2-Al_2O_3**	**Pd/ZrO_2**
μmol NH_3/g	197	213	241	280	399	460

* NH_3-TPD desorption profiles can be found in ESI (Figure S7).

3.2 Preliminary catalytic tests.

Initially, the reductive cyclo-amination of acetol with ethylenediamine was carried out (commercial catalyst) by arranging, from the beginning of the reaction, both reactants together with 1wt%Pd/Al_2O_3 (commercial catalyst) in the reactor under mild reaction conditions (at 90 ºC and P_{H_2} = 13 bar). In this case, methanol (MeOH) was used as solvent in order to avoid some negative effect of water during the dehydration intermediate step occurring during the process (see *Scheme 1*). The catalyst loading was varied from 0 to 35wt% with respect to the amine to maximize the yield to 2-methylpiperazine (2-MP). Under these conditions, maximum yields for 2-MP were achieved when using catalyst loadings from 25wt% onwards (Figure 4). A "plateau" effect occurs beyond this value, probably because of substrate limitations. The reaction product along with the different reaction intermediates and the by-products formed were identified by GC-MS (Figure S8-10, ESI).

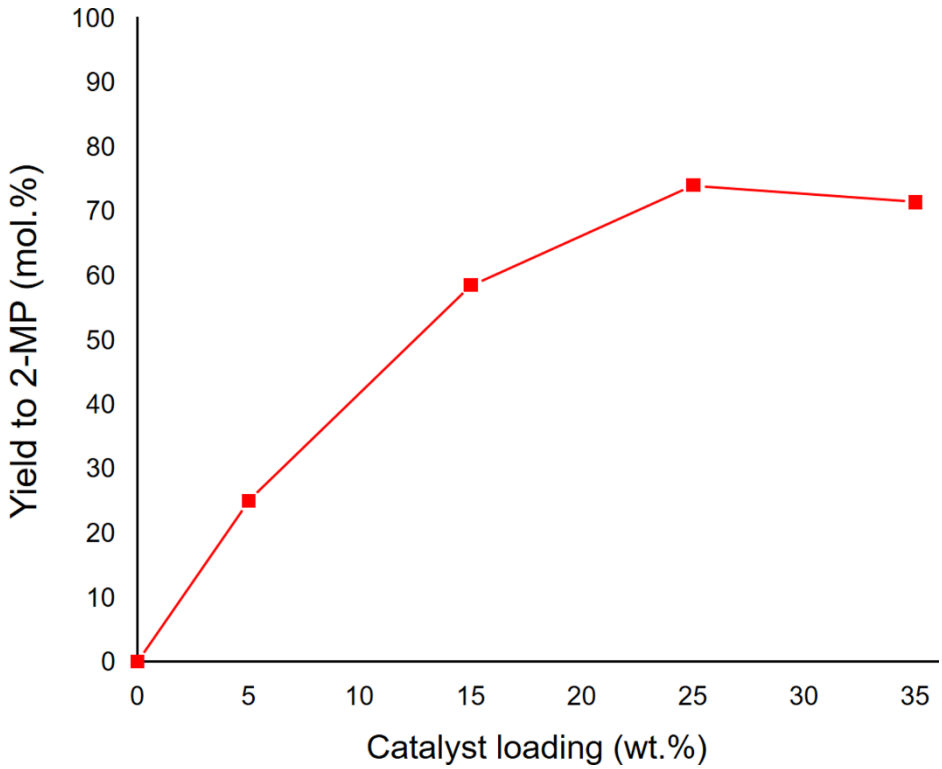

Figure 4. Catalyst loading optimization in the reductive cyclo-amination of acetol with ethylenediamine with 1wt%Pd/Al_2O_3 (commercial catalyst). Reaction conditions: 0.325 g acetol, 0.227 g ethylenediamine, 1.250 g MeOH, at 13 bar of H_2 and 90 ºC, during 7 h.

Aiming at increasing the yield to 2-MP, it was considered that slow acetol addition could be a key point to avoid secondary non-desired reactions as well as by-product formation. Results in Figure 5a clearly point out that slow addition of acetol leads to better ethylenediamine conversion values (>95%) when using Pd/Al_2O_3 commercial catalyst. The improvement in conversion could be explained considering that, with a large number of acetol molecules in the reaction mixture (situation with both reactants in the initial mixture), an ethylenediamine molecule would preferably react with two acetol molecules, by reaction between the carbonyl group of acetol and the terminal amines of the ethylenediamine, instead of reacting with the hydroxyl group of acetol, once the first nucleophilic addition has been completed (see Scheme 2). Therefore, considering that reactants were added in equimolar quantities (1:1), the formation of linear Nitrogen-containing by-products due to inter-molecular reactions between two acetol molecules and one ethylenediamine molecule are favored, thus leading to lower conversions and, therefore, lower yields of the desired 2-MP. On the contrary, slow addition of the acetol into the reaction mixture, strongly favors the intramolecular reaction, as illustrated in Scheme 2. Comparison of the selectivity values obtained for different reaction products at the same conversion level (isoconversion points, see ESI, Figure S12) for both standard and

slow acetol addition experiments, also demonstrates that a higher amount of Nitrogen-containing by-products (N-byproducts) can be observed in the case of the reaction started with equimolar amounts of acetol and ethylenediamine (Figure 5b). Quite the opposite, the selectivity is shifted towards the mixture comprising both, the 2-MP and its precursors (imine molecules) when acetol is slowly added into the reaction media.

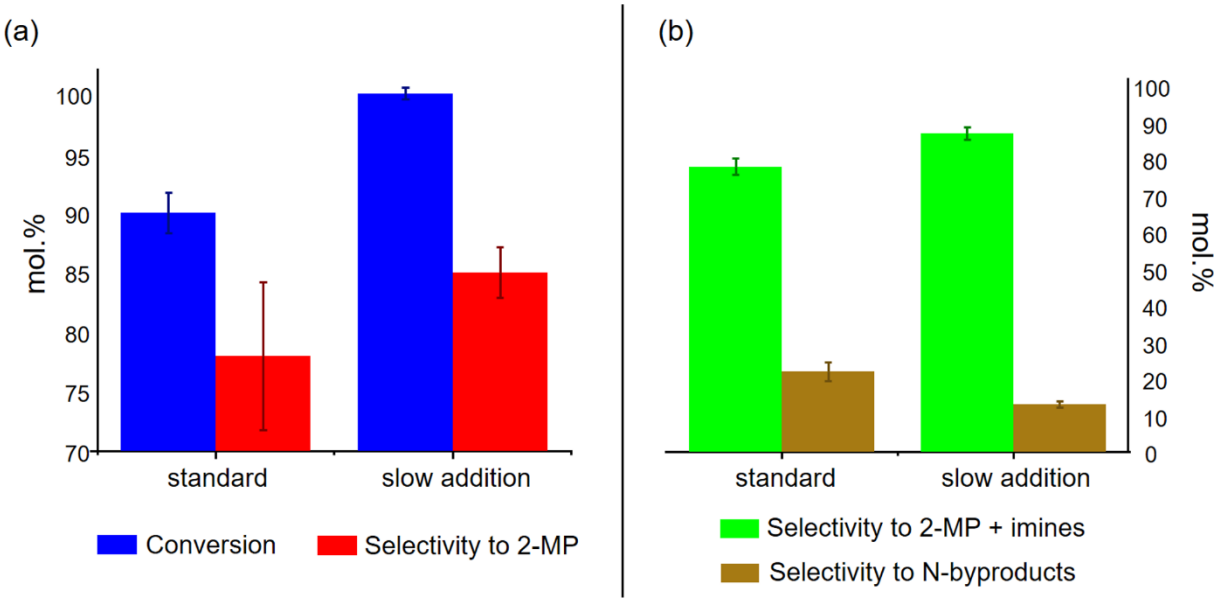

Figure 5. Effect of the slow addition of acetol to the reaction media in the reductive cyclo-amination of acetol with ethylenediamine over 1wt%Pd/Al_2O_3 (commercial catalyst). (a) Conversion and selectivity at 7 h. (b) Selectivity towards the different products compared at the same conversion level (time = 3h). Reaction conditions: 0.325 g acetol, 0.227 g ethylenediamine, 1.250 g MeOH, 0.056 g of catalyst, at 13 bar of H_2, and 90 ºC.

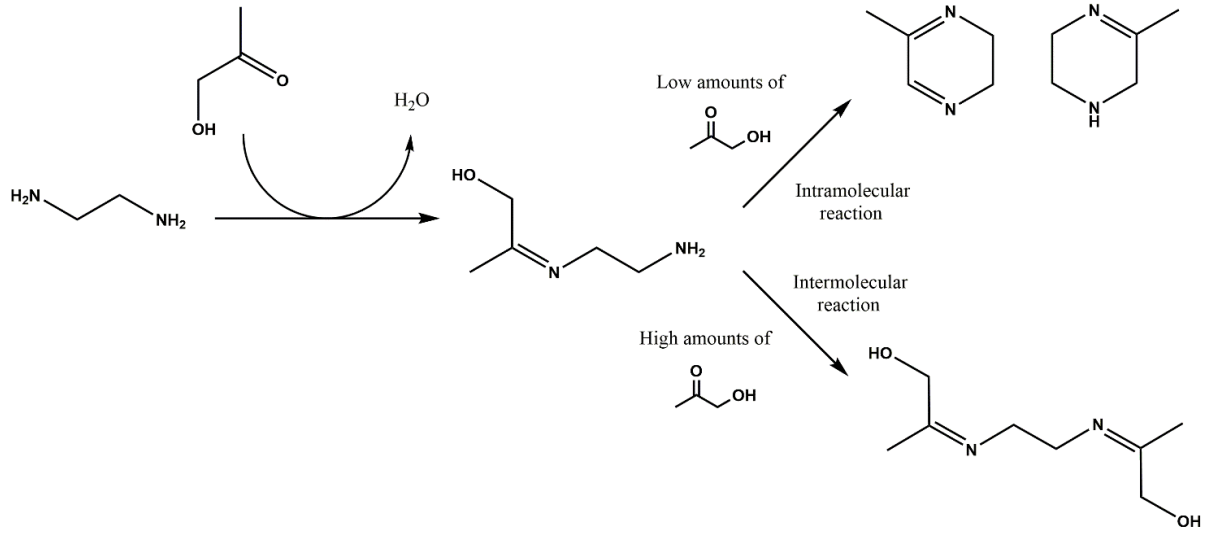

Scheme 2. Possible reaction pathways for the reductive cyclo-amination of acetol with ethylenediamine.

3.3 Catalytic activity of Pd supported on simple metal oxides.

Once the most appropriate reaction system for the reductive cyclo-amination of acetol with ethylenediamine by means of slow addition of acetol was determined, different Pd supported on simple metallic oxides prepared in this study were studied as catalysts, in order to maximize the yield towards the 2-MP desired product. The main results obtained are summarized in Table 3.

Table 3. Catalytic activity of Pd supported on simple metal oxide materials in the reductive cyclo-amination of acetol with ethylenediamine.

Catalyst	Ethylenediamine conversion (mol. %)		Selectivity to 2-MP (mol. %)		Yield to 2-MP (mol. %)*	
	1 h	7 h	1 h	7h	1 h	7 h
1.0wt%Pd/Al_2O_3 (commercial)	30	100	77	85	27	79
1.0wt%Pd/Al_2O_3	34	96	88	86	29	83
1.2wt%Pd/TiO_2	38	100	88	83	34	83
1.1wt%Pd/ZrO_2-mxt	38	99	80	82	30	79
1.0wt%Pd/MgO	41	94	81	81	33	76

Reaction conditions: 0.325 g acetol, 0.227 g ethylenediamine, 1.250 g MeOH, 0.056 g of catalyst, at 13 bar of H_2, and 90 ºC, during 7 h and with slow addition of acetol (100 µl/h). *Carbon balances for all reactions were higher than 95%.

Results prove that, independently of the support (Al_2O_3, ZrO_2, TiO_2 and MgO), Pd metallic species can carry out the reductive amination of acetol successfully. Nonetheless, the differences between them are hardly noticed, even at short reaction times, and more experiments should be done to further differentiate between these catalysts.

In order to make a difference between different catalysts, such as Pd/Al_2O_3, Pd/MgO, Pd/TiO_2 and Pd/ZrO_2, their stability after successive re-uses in the reaction was assessed. Bearing that objective in mind, the solids after reaction were recovered, washed with MeOH and used again in a new experiment. After several re-uses, they were regenerated and used as catalysts for an ultimate time. The procedure for re-uses and regeneration is more deeply described in Section

2.3. The results obtained (Figure 6) show the excellent stability of Pd/TiO_2 and Pd/ZrO_2 catalysts after three consecutive uses, while a decrease of around 10% was observed when using Pd/Al_2O_3 for the third time in a row. The Pd/MgO material, the only one with a basic character shows a higher deactivation by organic matter deposition during the reaction (Table 4), revealing the higher degree of polymerization reactions on the surface of this catalyst. This fact is in good agreement with what has been observed regarding side polymerization reactions in acetone and vinyl-ketones reaction systems.[40,41]

Regeneration enables almost complete elimination of the organic matter deposited on the solid and recovers the catalytic activity in the case of Pd/Al_2O_3. On the contrary, Pd/MgO seems not to be able to respond as well to the regeneration treatment, being yields to 2-MP notoriously lower than those corresponding to the first use. A more detailed structural analysis seeking to understand the effect of a second reduction on the properties of this material reveals that, even although the metal particle size does not increase after the regeneration of the used catalyst and palladium loading also remains constant (Table 4), a decrease in the crystallinity of MgO structure is observed (see ESI, Figure S13). This loss of crystallinity has been previously reported. Magnesia structure tends to collapse even in contact with air, and this may be affecting the catalytic properties.[42]

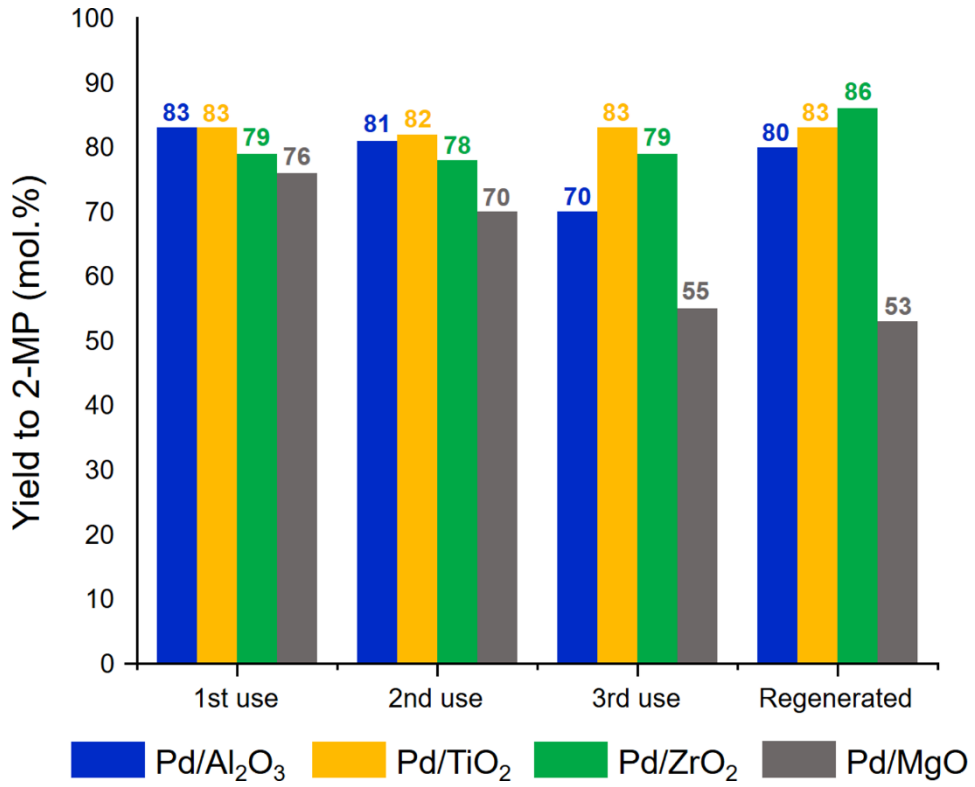

Figure 6. Catalyst re-usability and regeneration for Pd supported on simple oxide materials. Reaction conditions: 0.325 g acetol, 0.227 g ethylenediamine, 1.250 g MeOH, 0.056 g of catalyst, at 13 bar of H_2, and 90 ºC, during 7 h and with slow addition of acetol (100 µl/h).

Table 4. Effect of reusability and regeneration on organic matter deposition, metal loading and metallic dispersion of Pd supported on simple metal oxides.

Catalyst	Pd (wt.%)[a] [fresh]	Pd (wt%)[a] [after 1st use]	C/N (wt%)[b] [after 1st use]	C/N (wt%)[b] [after regeneration]	Pd particle size (nm)[c] [fresh]	Pd particle size (nm)[c] [after regeneration]
Pd/Al_2O_3	1.0	1.0	0.9/0.3	0.3/0.0	8	7
Pd/TiO_2	1.2	1.1	1.3/0.8	0.2/0.0	4	3
Pd/ZrO_2-mxt	1.1	1.0	1.3/0.3	0.3/0.0	5	4
Pd/MgO	1.0	1.0	5.8/0.7	0.8/0.3	14	13

[a] Pd content and chemical composition measured by ICP. [b] Results from elemental analyses (EA). [c] Average diameter of Pd nanoparticles calculated from TEM measurements of, at least, 100 particles.

Summarizing, good yields to 2-MP, with remarkably stability to the consecutive reuses, were encountered for Pd/TiO_2 and Pd/ZrO_2 type materials, with quite low organic matter deposition and practically no changes in metal oxide structure and Pd particle sizes, even after regeneration. In addition, although Pd/Al_2O_3 suffered some deactivation during re-uses, its catalytic activity is practically completely recovered after regeneration.

3.4 Catalytic activity of Pd supported on mixed metal oxides.

In view of the fact that Pd supported on Al_2O_3, TiO_2 and ZrO_2 catalysts produced the best results among all the tested catalysts in the reductive amination of acetol with ethylenediamine, especially when considering its resistance to deactivation over several uses, high surface area mixed oxides TiO_2-Al_2O_3, TiO_2-ZrO_2 and ZrO_2-Al_2O_3 were synthesized in this work, and Pd (≈1% in weight) was incorporated onto these materials by impregnation (See Table 1).

Kinetic curves for Pd-supported on metallic mixed oxide materials and compared with Pd-supported on simple oxides are provided in ESI (Figure S14). The Pd-supported mixed oxide catalysts presented higher catalytic activity than the respective materials based on simple oxides, increasing the values for the yield to 2-MP in 3 h of reaction from ≈75% to ≈85% (see ESI, Figure S14).

As in the case of Pd-supported on simple oxides, reusability and regeneration tests of Pd-supported on mixed oxides were performed to see if these materials could also keep their catalytic behavior during several cycles. Results in Figure 7 show that both, the consecutive re-uses and the regeneration process, do not significantly affect the catalytic performance of any of the prepared mixed oxides. Remarkably, Pd/TiO_2-ZrO_2 material show excellent stability (even after regeneration) followed by Pd/TiO_2-Al_2O_3 and Pd/ZrO_2-Al_2O_3 samples, respectively. These results are in agreement with what has been observed in the characterization analysis for the regenerated catalysts (Table 5) as, although the amount of organic matter deposited is higher than in the case of the catalysts based on simple oxides, this fact is likely to be compensated by the larger ~~area~~ amounts of active sites found in the materials described in this section (mainly due to the larger surface areas and the Pd particles with narrower size distributions and more centered at lower values observed for these samples). Nonetheless, and although the cleaning of the materials after the thermal regeneration is very satisfactory, it seems to be slightly affecting the catalytic performance in the cases of Pd/TiO_2-Al_2O_3 and Pd/ZrO_2-Al_2O_3, probably

because of the higher particle sizes observed after the regeneration process for these two catalysts (see Table 5 and Figure S6).

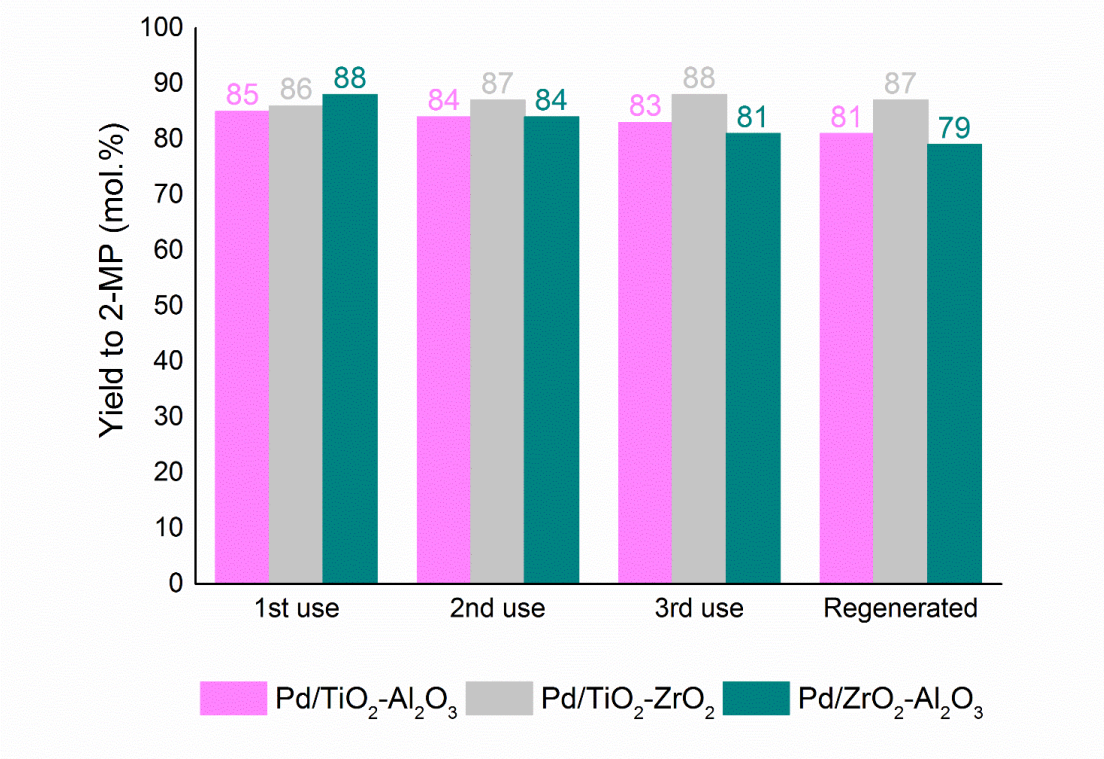

Figure 7. Catalyst re-usability and regeneration for Pd supported on mixed oxide materials. Reaction conditions: 0.325 g acetol, 0.227 g ethylenediamine, 1.250 g MeOH, 13 bar H_2, 0.056 g of catalyst at 90 ºC, during 7 h and with slow addition of acetol (100 µl/h).

Table 5. Effect of reusability and regeneration on organic matter deposition, metal loading and metallic dispersion of Pd supported on simple metal oxide.

Catalyst	Pd (wt.%)[a]		C/N (wt.%)[b]		Pd particle size (nm)[c]	
	[fresh]	[after 1st use]	[after 1st use]	[after regeneration]	[fresh]	[after regeneration]
Pd/TiO_2-Al_2O_3	1.0	1.0	2.7/1.2	0.8/0.3	1	4
Pd/TiO_2-ZrO_2	1.1	1.1	2.9/1.6	0.4/0.0	4	5
Pd/ZrO_2-Al_2O_3	1.0	0.9	2.5/0.7	0.4/0.1	4	6

[a] Pd content and chemical composition measured by ICP. [b] Results from elemental analyses (EA). [c] Average diameter of Pd nanoparticles calculated from TEM measurements of, at least, 100 particles.

3.5 Further comparison, understanding and catalyst selection.

With the aim of establishing a further differentiation between the three mixed oxides-supported Pd materials (i.e. Pd/TiO_2-Al_2O_3, Pd/TiO_2-ZrO_2, Pd/ZrO_2-Al_2O_3) and the other three simple oxides showing the best yields to 2-MP and also the capability of being reused and regenerated (i.e. Pd/TiO_2, Pd/Al_2O_3 and Pd/ZrO_2), a 3 h long reactions were carried out for each one by working with a very reduced amount of catalyst (0.011 g; 5wt% with respect to the amine). By doing this, the differences observed in previous sections (Figures 7 and S14) were supposed to be made much clearer. Additionally, Table S3 shows how the "effective activity of the catalyst" (Yield to 2-MP, see *Section 2.4*) has always been kept far below 90%.

Data of Table 6 indicate that Pd/TiO_2-Al_2O_3 was, in fact, the material intrinsically more active among those studied in this work (Yield to 2-MP = 57%), followed by Pd/ZrO_2-Al_2O_3 (Yield to 2-MP = 49%). In addition to these experiments, the acid properties of the different Pd-supported materials here studied were determined by adsorption-desorption experiments with ammonia (NH_3-TPD measurements, see Experimental section). A correlation between the catalytic activity (in terms of Yield to 2-MP) and the total Lewis acidity (examined by NH_3-TPD) of the Pd-supported materials was established and depicted in Figure 8, where results point out Pd/ZrO_2-Al_2O_3 and Pd/TiO_2-Al_2O_3 as the two materials with the highest 2-MP production values.

Table 6. Yield to 2-MP and TON in the reductive cyclo-amination of acetol with ethylenediamine at shorter reaction times and with lower catalyst loadings.

Catalyst	**Pd/Al_2O_3**	**Pd/TiO_2-ZrO_2**	**Pd/ZrO_2-mix.**	**Pd/TiO_2**	**Pd/ZrO_2-Al_2O_3**	**Pd/TiO_2-Al_2O_3**
Yield to 2-MP (mol.%)	23	26	29	44	49	57
TON[a]	818	841	938	1304	1937	2028

Reaction conditions: 0.325 g acetol, 0.227 g ethylenediamine, 1.250 g MeOH, 0.011 g of catalyst at 90 ºC and 13 bar of H_2, during 3 h and with slow addition of acetol (100 µl/h). [a] TON = mol 2-MP·mol Pd^{-1}.

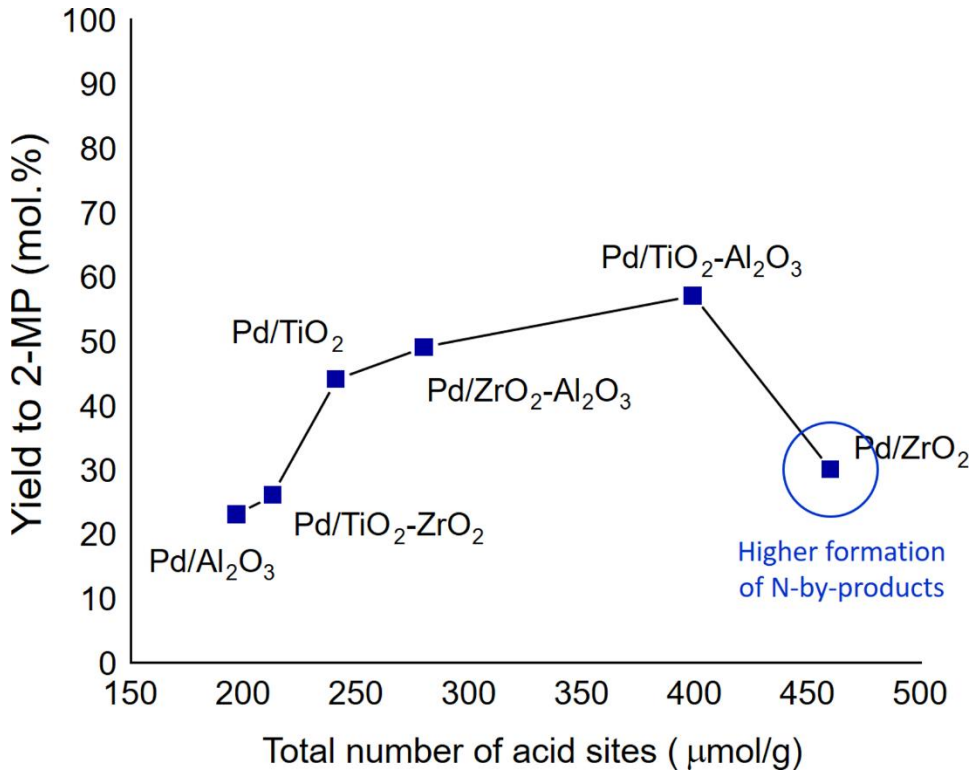

Figure 8. Yield to 2-MP as a function of the total number of Lewis acid sites for Pd-supported materials in the reductive cyclo-amination of acetol with ethylenediamine. Reaction conditions: 0.325 g acetol, 0.227 g ethylenediamine, 1.250 g MeOH, 0.011 g of catalyst, at 90 ºC and 13 bar of H_2, during 3 h and with slow addition of acetol (100 µl/h).

Nevertheless, the explanation to this tendency with respect to the total number of Lewis acid sites is not straightforward and, therefore, the acidity seems not to be enough as to fully understand the reactivity in this series of materials. A detailed analysis of the product distribution for the different materials unveiled that high concentrations of acid sites shift the selectivity towards the appearance of non-desired Nitrogen-containing by-products (see ESI, Table S3). However, the reason why low concentrations of acid sites are detrimental for achieving high yields to 2-MP is not clear. Acid sites are often described in the literature to be a key point to favor the imine intermediate.[43] However, the formation of the imine intermediates seems to happen regardless of the support used, that is to say, at both ends of the graph (Figure 8), also occurring without catalyst, and even in the absence of hydrogen (see ESI, Table S3). On the other hand, no significant amounts of Nitrogen-containing by-products (N-by-products different from imines) are observed for any material apart from Pd/ZrO_2 (see ESI, Table S3).

Consequently, and on the account of the fact that differences in the imine hydrogenation are mainly what is defining the activity dissimilarities between catalysts (see ESI, Table S3), a greater deal of attention must be paid to hydrogen activation and C=N bond activation. Therefore, an analysis of the particle morphology together with the ability of each one of the catalysts to activate molecular H_2 has been performed in order to cogently explain the catalytic differences. Therefore, IR spectroscopy of CO adsorption as probe molecule and H_2/D_2 isotopic exchange experiments have been performed in order to analyse the surface metal sites (i.e. crystal facets, uncoordinated sites, and particle morphology) and the H_2 activation on the studied catalysts. In this sense, the recent literature on hydrogenation processes via metal nanoparticles has called attention to the role of the preferential activation of certain functional groups on specific metal nanoparticle features (i.e. facets, terraces, defects).[35,36,44] Concretely, in the work of Vidal et al [35] uncoordinated surface sites in Pt/TiO_2 catalysts have been proposed as chemoselective for the hydrogenation of the imine (C=N) group. In fact, in our work, by performing IR of CO adsorption studies, unsaturated sites characterized by an IR band of the Pd-CO interaction at 2042 cm^{-1}, have been predominately observed in the Pd/TiO_2-Al_2O_3 sample (Fig. 9, red line) and in less extension in the Pd/ZrO_2-Al_2O_3 sample (Fig. 9, green line). In addition, (111) and (100) facets (IR band at 2092 and 2085 cm^{-1}) together with bridge CO and 3-fold CO configuration on Pd terraces (IR band at 1988 and 1925 cm^{-1}, respectively) are also observed, but being more dominant in the Pd/TiO_2 and Pd/Al_2O_3 samples (Fig. 9, black and blue lines, respectively).[45-48] Thus, based on the IR-CO results and correlating them with the catalytic data of Table 6, it is likely that uncoordinated Pd sites as in the Pd/TiO_2-Al_2O_3 sample favour imine hydrogenation. Moreover, these sites are more abundant at smaller particle sizes, as is the case of the Pd supported on bimetallic oxide catalysts. On the other hand, H_2 activation seems not to be determinant in catalyst activity since, based on the H_2/D_2 isotopic exchange experiments (Table 7 and Fig. S15-S18), similar H_2 activation ability is observed on all samples.

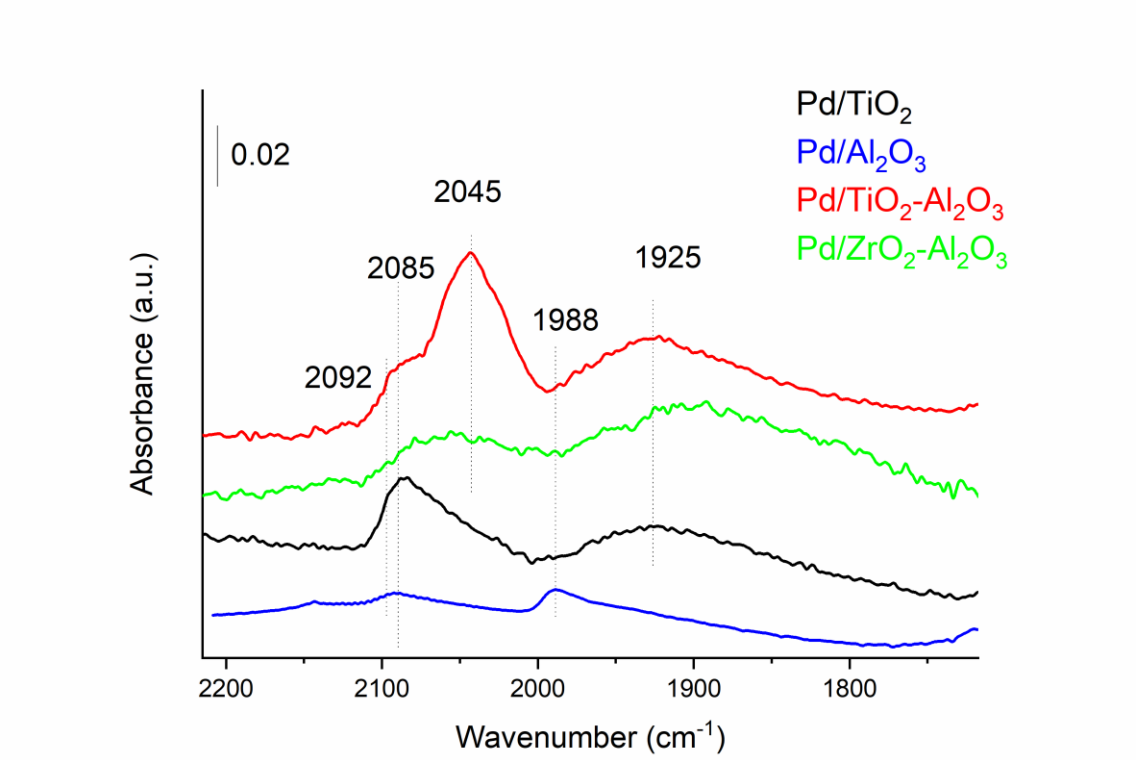

Figure 9. IR spectra of CO adsorption at saturation coverage (i.e. 8.5 mbar CO) on Pd supported catalysts (after reduction).

Table 7. HD/H_2 mass signal ratio during the H_2/D_2 experiments over Pd-supported catalysts at different temperatures.

Catalyst	HD (T) / H_2-bypass			
	25 ºC	**60 ºC**	**90 ºC**	**120 ºC**
Pd/Al_2O_3	0.40	0.48	0.51	0.54
Pd/TiO_2-Al_2O_3	0.21	0.32	0.38	0.43
Pd/ZrO_2-Al_2O_3	0.26	0.39	0.45	0.50

After these findings, the superior catalytic performance of Pd/TiO_2-Al_2O_3 and Pd/ZrO_2-Al_2O_3 could be explained. Nevertheless, and in order to select one of the two Pd-supported materials for further catalytic activity studies, a kinetic comparison between Pd/TiO_2-Al_2O_3 and Pd/ZrO_2-Al_2O_3 was also done, verifying that, in fact, both catalysts show quite similar results in every section of the kinetic curve (see Figure S19, ESI). At this point, and although Pd/TiO_2-Al_2O_3

could be selected as the best catalyst by taking into account its higher TON (see Table 6), two main reasons for its selection can be stated: i) its slightly higher reusability and regeneration capacity (see section 3.4), and ii) the inexpensive character of the Ti precursor in comparison with the Zr precursor used in catalyst preparation is enough reason.

3.6 Reusability of Pd/TiO_2-Al_2O_3, use in water and extension to other reactants

With the idea to increase catalytic applicability in the process for 2-MP synthesis from acetol and considering the excellent performance of Pd/TiO_2-Al_2O_3 catalyst, the possibility to achieve high yields to 2-MP with low catalyst loadings (5 wt% with respect to the amine) was checked, also testing the reusability of the catalyst when working under these affordable reaction conditions. Figure 10 shows that it is possible to attain 2-MP yields close to 80% with Pd/TiO_2-Al_2O_3 at 7 h of reaction, even when working with low amounts of catalyst. However, an undeniable loss of activity over the successive reuses is observed. This was expected since now the deposition of organic matter on the catalytic surface is taking more importance, as the elemental analysis studies unveiled (see ESI, Table S4). Nonetheless, it is possible to clean the catalytic surface and practically recover the catalytic activity after a regeneration process (Figure 10, Table S4). Importantly, when doing so, the average size of Pd particles on the catalyst is slightly increased (Figure S6a), which may account for this moderate-to-low loss of activity.

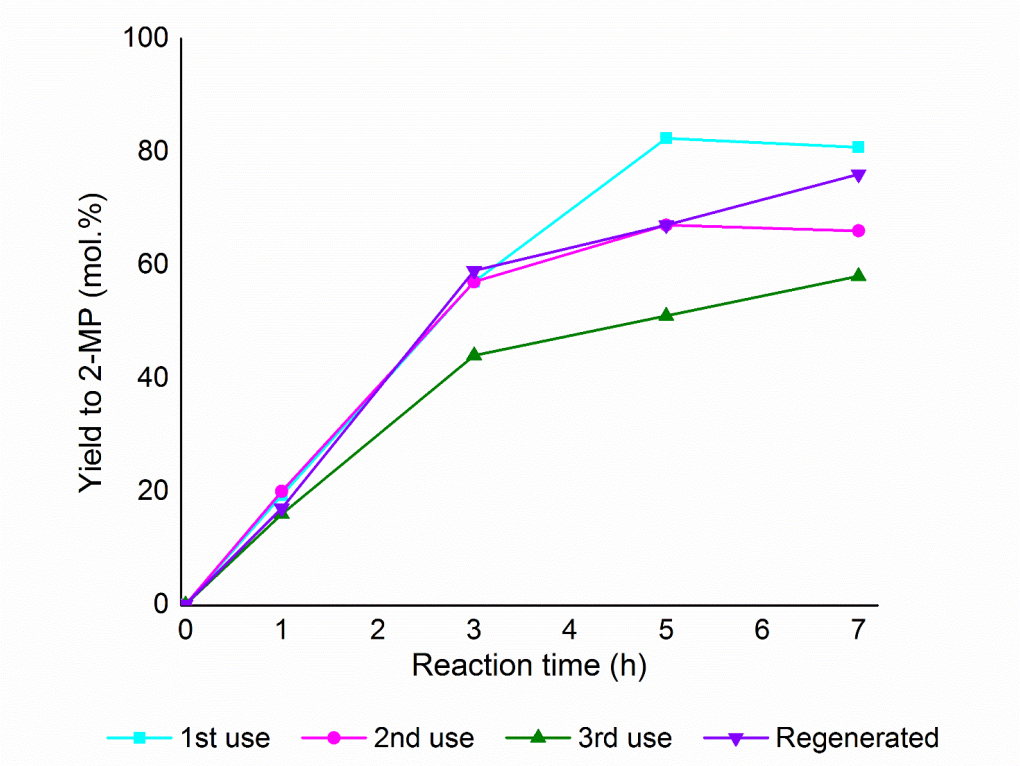

Figure 10. Yield to 2-MP in the reductive cyclo-amination of acetol with ethylenediamine with Pd/TiO_2-Al_2O_3 over three consecutive catalytic cycles and the regenerated catalyst. Reaction conditions: 0.325 g acetol, 0.227 g ethylenediamine, 1.250 g MeOH, 0.011 g of catalyst, at 90 ºC and 13 bar of H_2, during 7 h and with slow addition of acetol (100 µl/h).

Finally, the possibility of using this catalyst in aqueous systems and for other reductive amination reactions with different carbonyl-type compounds derived from biomass feedstocks could be of industrial interest. For instance, glyoxal (1,2-ethanedial) could be an excellent candidate to be used as a starting reactant. This highly reactive dialdehyde offers numerous alternatives for reductive amination processes, either with amines[49] or amino acids[50], as a source of amino groups, and it can be produced from either biomass[51] or ethylene glycol oxidation[52,53]. The synthetic possibilities for glyoxal and amines in an aqueous medium are diverse and they would include compounds of interest such as: N,N'-diisopropyl-ethylendiamine, N,N′-acetic acid-ethylenediamine (EDTA), amongst others, with current troublesome synthesis implying either several reaction stages or the use of classic reductive agents.

In our case, the catalytic experiments were performed by using glyoxal and tert-butylamine (as N source), carrying out imination and hydrogenation reactions in a single step, with commercial Pd/Al_2O_3 and Pd/TiO_2-Al_2O_3 as catalysts. Since most of the already described reductive

aminations involving glyoxal use water as solvent, a test was done with acetol and ethylenediamine to see to what extent using water instead of MeOH would be detrimental for the catalytic performance. The results are summarized in Figure 11.

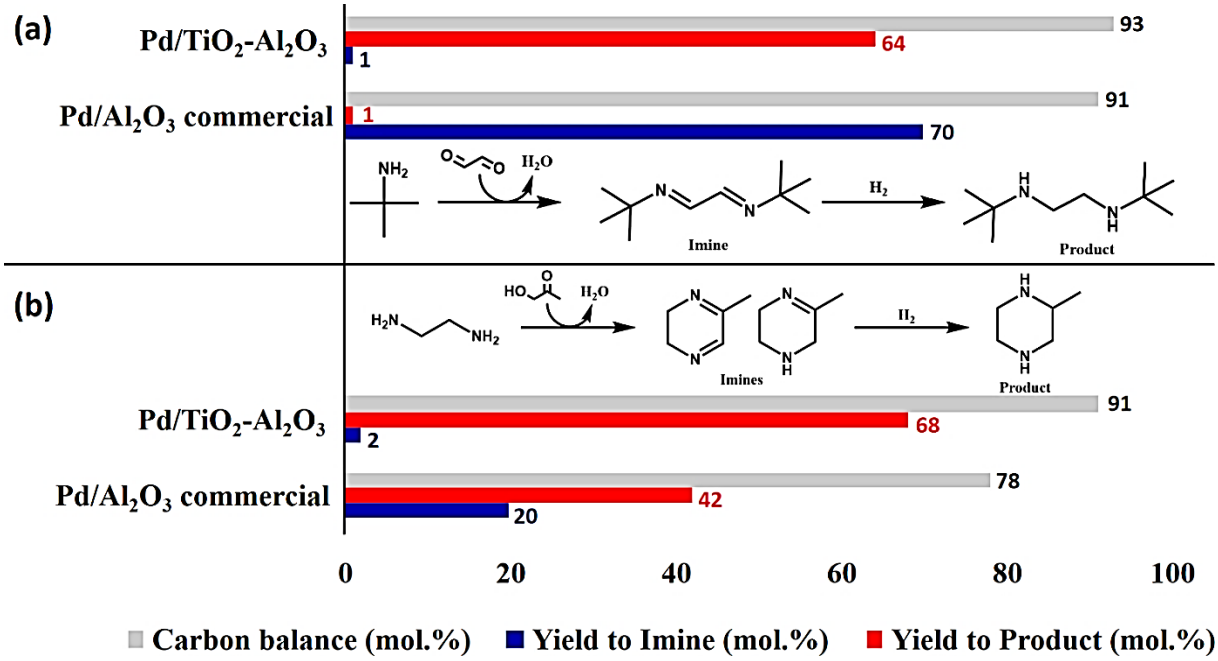

Figure 11. Reductive amination with glyoxal and tert-butylamine over 1%Pd/Al_2O_3 (commercial catalyst) and 1%Pd/TiO_2-Al_2O_3 material. Reaction conditions: (a): 0.550 g tert-butylamine, 0.430 ml glyoxal, 0.500 g H_2O (40% ac, slow addition = 140 µl//h), 0.135 g of catalyst, at 90 ºC and 15 bar of H_2, during 4 h. (b) 0.325 g acetol, 0.227 g ethylenediamine, 1.250 g H_2O, 13 bar H_2, 0.011 g of catalyst at 90 ºC, during 7 h and with slow addition of acetol (100 µl/h).

Figure 11 clearly shows how our catalyst works better in water than the commercial Pd/Al_2O_3 in the 2-methylpiperazine synthesis and, specially, in the reductive amination with glyoxal and tert-butylamine. Thus, 64% yield of the desired N-compound synthesized form glyoxal was attained with the Pd/TiO_2-Al_2O_3 catalyst, whilst very low amounts of the product were detected with the Pd-based commercial catalyst. Besides, 68% yield to 2-MP was achieved by using the Pd-supported mixed oxide catalyst instead of the 42% yield reached with Pd/Al_2O_3. These evidences further confirm the greater capability of Pd/TiO_2-Al_2O_3 to hydrogenate the C=N functionality. It is also observed that carbon balances in water decrease when compared to that reactions carried out in MeOH (>95% in both cases). This fact is also proven by elemental analyses (see Table S4), and this is likely to lead to a more important deactivation. Nonetheless, the much better result obtained for the glyoxal reaction with Pd/TiO_2-Al_2O_3 allows us to think

that it is quite feasible to carry out this sort of reactions with high yields of the desired Nitrogen-compounds by using this catalyst under mild reaction conditions affordable at industrial scale.

4. Conclusions

A new and efficient catalytic route involving the reductive cyclo-amination of acetol with ethylenediamine in order to obtain 2-methylpiperazine (2-MP) can be carried out by using a series of solid catalysts based on Pd nanoparticles supported on simple and mixed metal oxides, easy and economical to be prepared, under mild reaction conditions. 2-MP yield optimization and catalyst stability studies have been carried out, being Pd/TiO_2, Pd/ZrO_2, Pd/TiO_2-Al_2O_3, Pd/TiO_2-ZrO_2 and Pd/ZrO_2-Al_2O_3 the materials that presented the best results in terms of activity and reusability among all the tested materials. Moreover, Pd/TiO_2-Al_2O_3 showed higher activity than any other catalyst, being able to carry out the reaction either in shorter times or with very low catalyst loadings (≈5wt%). The correlation between the total number of acid sites with the yield to 2-MP stablished that too many acid sites resulted in the formation of more non-desired Nitrogen-containing by-products. On the other hand, a particle morphology exposing a large number of unsaturated Pd sites is essential to activate the C=N double bond and enhance its hydrogenation, as presented specially on Pd/TiO_2-Al_2O_3. Finally, the scope extension of Pd/TiO_2-Al_2O_3 catalyst was assessed, thus proving to be capable to work properly when using other reductive amination substrates and at different conditions. Despite some moderate-to-low catalytic deactivation occurring when reactions are carried out in aqueous media, the catalytic activity continues to be good independently of the reactants employed. These findings make possible to think about future reductive amination processes in aqueous systems or involving a mixture of solvents by using this Pd-supported on mixed oxide as catalyst.

5. Acknowledgements

The authors express their gratitude to the Spanish Government for the funding (MICINN: CTQ2015-67592, PGC2018-097277-B-I00 and Severo Ochoa Program: SEV-2016-0683). J.M. thanks the MICINN (CTQ2015-67592) for his PhD scholarship. Z.R. thanks the Islamic Center Association for Guidance and Higher Education for his PhD scholarship. Authors also thank the Electron Microscopy Service of Universitat Politècnica de València for their support and M. Parreño-Romero for her assistance with the measurements.

6. Conflicts of interest

There are no conflicts to declare.

7. References

[1] M. Stöcker, *Angew. Chem. Int. Ed.*, 2008, **47**, 9200-9244. https://doi.org/10.1002/anie.200801476

[2] G.W. Huber, S. Iborra and A. Corma, *Chem. Rev.*, 2006, **106**, 4044-4098. https://doi.org/10.1021/cr068360d

[3] Y. Wang, S. Furukawa, X. Fu and N. Yan, *ACS Catal.*, 2020, **10**, 311−335. https://pubs.acs.org/doi/10.1021/acscatal.9b03744.

[4] S. Sato, M. Akiyama and R. Takahashi, *Appl. Catal. A: Gen.*, 2008, **347**, 186-191. https://doi.org/10.1016/j.apcata.2008.06.013

[5] M. Velasquez, A. Santamaria and C. Batiot-Dupeyrat, *Appl. Catal. B: Environ*., 2014, **160**, 606-613. https://doi.org/10.1016/j.apcatb.2014.06.006

[6] S. Celerier, S. Morisset, I. Batonneau-Gener, T. Belin, K. Younes and C. Batiot-Dupeyrat, *Appl. Catal. A: Gen*., 2018, **557**, 135-144. https://doi.org/10.1016/j.apcata.2018.03.022

[7] J. Mazarío, P. Concepción, M. Ventura and M.E. Domine, *J. Catal*., 2020, **385**, 160-175. https://doi.org/10.1016/j.jcat.2020.03.010

[8] P. Anastas and N. Eghbali, *Chem. Soc. Rev*., 2010, **39(1)**, 301-312. https://doi.org/10.1039/B918763B

[9] R. J. Martin. *VET J*., 1997, **154**, 11–34. https://doi.org/10.1016/S1090-0233(05)80005-X

[10] R.D. Taylor, M. MacCoss and A.D. Lawson, *J. Med. Chem*., 2014, **57**, 5845-5859. https://doi.org/10.1021/jm4017625

[11] G.T. Rochelle, *Science*, 2009, **325**, 1652-1654. https://doi.org/10.1126/science.1176731

[12] S.A. Freeman, R. Dugas, D.H. Van Wagener, T. Nguyen and G.T. Rochelle, *Int. J. Greenhouse Gas Control*, 2010, **4**, 119-124. https://doi.org/10.1016/j.ijggc.2009.10.008

[13] R.D. Ashford, Ashford's Dictionary of Industrial Chemicals, third ed., Wavelength Publications, Saltash, 2011.

[14] E.-L. Dreher, K.K. Beutel, J.D. Myers, T. Lübbe, S. Krieger and L. H. Pottenger, in: Ullmann's Encyclopedia of Industrial Chemistry, Wiley-VCH, Weinheim, 2014.

[15] K. Weissermel, H.-J. Arpe, C. R. Lindley and S. Hawkins, in: Industrial Organic Chemistry. Wiley-VCH, 2003, pp. 159–161.

[16] L.J. Kitchen and C.B. Pollard, *J. Am. Chem. Soc.*, 1947, **69**, 854-855. https://doi.org/10.1021/ja01196a034

[17] G. Bai, X. Fan, H. Wang, J. Xu, F. He and H. Ning, *Catal. Commun*., 2009, **10**, 2031-2035. https://doi.org/10.1016/j.catcom.2009.07.025

[18] C.M. Subrahmanyam, G. Muralidhar, S. J. Kulkarni, V. Viswanathan, B. Srinivas, J. S. Yadav and A.V. Rama Rao, Ind. Pat., 281/DEL/92, 1992.

[19] N. Narender, P. Srinivasu, S.J. Kulkarni and K.V. Raghavan, *J. Catal.*, 2001, **202**, 430-433. https://doi.org/10.1006/jcat.2001.3291

[20] K. Nagaiah, A.S. Rao, S.J. Kulkarni, M. Subrahmanyam and A.R. Rao, *J. Catal*., 1994, **147**, 349-351. https://doi.org/10.1006/jcat.1994.1147

[21] R.B. Chedid, J-P. Melder, U. Abel, R. Dostalek, N. Challand, B. Stein and M. Jödecke, BASF SE, US Pat. 8981093B2, 2015.

[22] M.E. Domine, M.C. Hernández-Soto, M.T. Navarro and Y. Pérez, *Catal. Today*, 2011, **172**, 13-20. https://doi.org/10.1016/j.cattod.2011.05.013

[23] M.E. Domine, M.C. Hernández-Soto and Y. Pérez, *Catal. Today*, 2011, **159**, 2-11. https://doi.org/10.1016/j.cattod.2010.08.011

[24] H. Blaser, U. Siegrist, H. Steiner, M. Studer, R. Sheldon and H. van Bekkum, Fine chemicals through heterogeneous catalysis, first ed., Wiley/VCH, Weinheim, 2001.

[25] A. Baiker and J. Kijenski, *Catal. Rev. Sci. Eng.*, 1985, **27**, 653-697. https://doi.org/10.1080/01614948508064235

[26] E.W. Baxter and A.B. Reitz, *Org. Reactions*, 2002, **59**, 1-714. https://doi.org/10.1002/0471264180.or059.01

[27] A. Pelter, R.M. Rosser and S. Mills, *J. Chem. Soc., Perkin Trans.*, 1984, **1**, 717-720. https://doi.org/10.1039/P19840000717

[28] A.F. Abdel-Magid and S.J. Mehrman, *Org. Process Res. Dev*., 2006, **10**, 971-1031. https://doi.org/10.1021/op0601013

[29] L. Rubio-Pérez, F.J. Pérez-Flores, P. Sharma, L. Velasco and A. Cabrera, *Org. Lett.*, 2008, **11**, 265-268. https://doi.org/10.1021/ol802336m

[30] D. Imao, S. Fujihara, T. Yamamoto, T. Ohta and Y. Ito, *Tetrahedron*, 2005, **61**, 6988-6992. https://doi.org/10.1016/j.tet.2005.05.024

[31] S. Enthaler, *ChemCatChem*, 2010, **2**, 1411-1415. https://doi.org/10.1002/cctc.201000180

[32] N.R. Candeias and C.A.M. Afonso, *J. Mol. Catal. A: Chem*., 2005, **242**, 195-217. https://doi.org/10.1016/j.molcata.2005.07.042

[33] S. Shimizu, T. Niwa and T. Shoji, Koei Chemical Co. Ltd., Jap. Pat. 02011577, 1988.

[34] U. Dingerdissen and W. Hoelderich, BASF SE, US Pat. 5290932A, 1991.

[35] A. Corma, T. Ródenas and M.J. Sabater, *Chem. Eur. J*., 2010, **16(1)**, 254-260. https://doi.org/10.1002/chem.200901501

[36] J.D. Vidal, M.J. Climent, P. Concepción, A. Corma, S. Iborra and M.J. Sabater, *ACS Catal*., 2015, **5**, 5812-5821. https://doi.org/10.1021/acscatal.5b01113

[37] A. García-Ortiz, J.D. Vidal, M.J. Climent, P. Concepción, A. Corma and S. Iborra, *ACS Sustainable Chem. Eng.*, 2019, **7**, 6243−6250. https://doi.org/10.1002/cssc.201601333

[38] A.S. Touchy, S.M.A. Hakim Siddiki, K. Kon and K.I. Shimizu, *ACS Catal*., 2014, **4**, 3045-3050. https://doi.org/10.1021/cs500757k

[39] S. Wei, Z. Dong, Z. Ma, J. Sun and J. Ma, *Catal. Commun*., 2013, **30**, 40-44. https://doi.org/10.1016/j.catcom.2012.10.024

[40] W. Ueda, T. Yokoyama, Y. Moro-Oka and T. Ikawa, *J. Chem. Soc., ChemCommun.*, 1984, **1**, 39-40. https://doi.org/10.1039/C39840000039

[41] N.E. Fouad, P. Thomasson and H. Knözinger, *Appl. Catal. A: Gen*., 2000, **194**, 213-225. https://doi.org/10.1016/S0926-860X(99)00369-5

[42] H. Hattori, *Chem. Rev.*, 1995, **95**, 537. https://doi.org/10.1021/cr00035a005

[43] G. Liang, A. Wang, L. Li, G. Xu, N. Yan and T. Zhang, *Angew. Chem. Int. Ed.*, 2017, **56**, 3050-3054. https://doi.org/10.1002/anie.201610964

[44] J. Mazarío, M. Parreño-Romero, P. Concepción, M. Chávez-Sifontes, R.A. Spanevello, M.B. Comba, A.G. Suárez and M.E. Domine, *Green Chem.*, 2019, **21**, 4769-4785. https://doi.org/10.1039/C9GC01857C

[45] H. Borchert, B. Jürgens, V. Zielasek, G. Rupprechter, S. Giorgio, C.R. Henry and M. Bäumer, *J. Catal.*, 2007, **247**, 145-154. https://doi.org/10.1016/j.jcat.2007.02.002

[46] D. Tessier, A. Rakai and F. Bozon-Verduraz, *J. Chem. Soc. Faraday Trans*., 1992, **88(5)**, 741-749. https://doi.org10.1039/FT9928800741

[47] S. Bertarione, D. Scarano, A. Zecchina, V. Johanek, J. Hoffmann, S. Schauermann, M.M. Frank, J. Libuda, G. Rupprechter and H.J. Freund, *J. Phys. Chem. B*, 2004, **108**, 3603-3613. https://doi.org/10.1021/jp036718t

[48] D. Ferri, C. Mondelli, F. Krumeich and A. Baiker, *J. Phys. Chem. B*, 2006, **110(46)**, 22982-22986. https://doi.org/10.1021/jp065779z

[49] H. Mueller and W. Mesch, BASF SE, US Pat. 4792631A, 1987.

[50] D.A. Bassett and E.L.M. Cowton, Innospec Ltd, Ep. Pat. 0820430B1, 1996.

[51] K.H. Oehr and J. Mckinley, in: Bridgwater A.V. (Eds.) Advances in Thermochemical Biomass Conversion, Springer, Dordrecht, 1993, pp. 1452-1455

[52] J.B. Trecek and G.L. Wiesner, Freedom Textile Chemicals Co, US Pat. 4258216A, 1979.

[53] Y. Toyoda, K. Wakimura, T. Hase and N. Arashiba, Mitsui Toatsu Chemicals Incorporated, Mitsui Chemicals Inc, US Pat. 4555583A, 1983.